Turkish Journal of Electrical Engineering & Computer Sciences

http://journals.tubitak.gov.tr/elektrik/

Research Article

Turk J Elec Eng & Comp Sci
(2017) 25: 2522 – 2534

doi:10.3906/elk-1605-307

# Safety-critical wireless sensor networks under a polyphase spreading sequences scenario

**Poonam GOYAL***, **Brahmjit SINGH**
Department of Electronics and Communication Engineering, National Institute of Technology Kurukshetra, Kurukshetra, India

**Received:** 26.05.2016 • **Accepted/Published Online:** 20.09.2016 • **Final Version:** 29.05.2017

**Abstract:** Reliable communication is a vital issue for safety- and mission-critical wireless sensor network environments such as industrial monitoring, medical care, and battlefield surveillance. These networks require highly accurate and delay-intolerant wireless communications. Under such critical conditions, the chip sequences used in these networks become vulnerable because of channel impairments and other interferences, thereby significantly decreasing overall system performance. In this paper, polyphase sequences are employed at the physical layer of IEEE Standard 802.15.4 to enhance the communication reliability of wireless sensor networks. Through an extensive simulation, it is found that upon applying polyphase sequences, the chip errors are reduced to $2.94 \times 10^{-6}$ in comparison to $1.18 \times 10^{-5}$ of conventional binary sequences (PN sequences).

**Key words:** Chip sequences, aperiodic autocorrelation function, aperiodic cross-correlation function, chip error rate

## 1. Introduction

Wireless sensor networks (WSNs) are distributed networks made up of large numbers of sensor nodes. They have the capabilities of sensing, processing, storing, and communicating with the centralized processing station and other sensor nodes. These sensor nodes are deployed randomly in harsh environments to sense various physical properties such as temperature, motion, air pressure, light intensity, and electromagnetic radiations. The WSN communication architecture consists of sensor nodes, a sink node, and a user node, as shown in Figure 1 [1,2]. Sensor nodes do not directly transfer the raw data to the user nodes; instead, they carry out computations on the data and then transmit only the required data to the sink node. The sink node then communicates the useful information to the user node via the Internet or satellite communication. These sensor nodes form the communication backbone of WSNs, which can be utilized by the other resource-constrained sensor devices to reach the base station. The application of these networks is found in the military, including battlefield surveillance, nuclear and chemical attack detection, medical disease diagnosis, and drug management, as well as in environmental monitoring such as forest fire detection and flood detection [3–5].

WSNs used for safety-critical applications such as industrial monitoring, minelaying, or healthcare and similarly for mission-critical programs including battlefield surveillance, and intrusion detection face the primitive issues of communication reliability and energy efficiency [4,5]. In these WSNs, communication must be error-free and delay-intolerant. However, in the case of classical WSNs, such as those used in agriculture, environment monitoring, or target tracking, the sensor readings are updated on the order of minutes/hours or

*Correspondence: poonamg1989@gmail.com

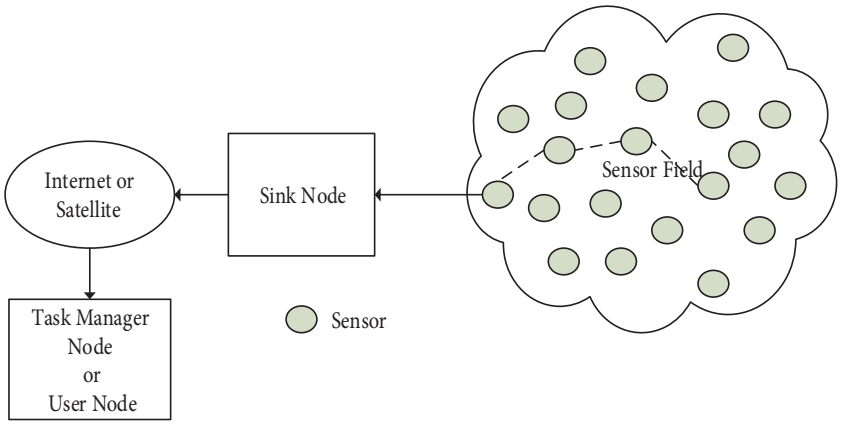


**Figure 1.** Sensors network architecture.

sometimes days. The delayed delivery of such types of measurements is not a major problem, because loss of data does not cause any harm to the environment. On the other hand, in the case of industrial WSNs, the loss of a few data packets may be hazardous for machines, the environment, and human lives as well. For this reason, in these WSNs, the transmission of a new sensor value is favored over retransmission of an erroneous value [6].

The IEEE standard used for WSNs is IEEE 802.15.4, which specifies only the physical layer and medium access control (MAC) layer. The physical layer employs the direct sequence spread spectrum (DSSS) technique for making the transmitting signal appear as noise, therefore increasing the signal robustness to noise and interference. In the DSSS, the information bits are divided into small pieces known as chips, which are then transmitted to a frequency channel over the spectrum. The information signal is combined with a high data rate bit sequence, known as a chip sequence or spreading sequence [6–8]. The chip level information is more informative than the bit level information. At the receiver end, chip-to-bit mapping is an approximation where valuable channel information is more prone to error. Various commercial off-the-shelf (COTS) motes, e.g., Rene, Mica2, and Mica2Dot, use the chip error rate of a few physical header bytes to improve the link quality of the signal.

The communication errors propagate from the chip to the bit level and then at the packet level. Therefore, the first step is to minimize the errors at the chip level. The chip errors can be reduced by redesigning the chip sequences that are already in use. In [9,10], PN sequences were used as standard chip sequences. These sequences were used to replace 4 bits of information (known as symbols) by chipping sequence of length 32. Similarly, Gold codes are widely employed at the DSSS physical layer of the IEEE 802.15.4k Standard used for low-energy critical infrastructure monitoring (LECIM) networks. LECIM networks find their application in transportation systems, oil and gas product production, water leak detection, inventory control, etc. Gold codes are used inside a co-located orthogonal network in LECIM systems [11–13]. However, these codes are prone to errors in real-time transmissions. To solve this problem, a 7-repetition code (RC7) was proposed by Barac et al. in [6]. RC7 codes provide the lowest possible computational complexity and substantial improvement in chip errors.

In safety-critical applications of WSNs, such as in medical applications, in order to examine the health of a patient continuously, the various sensors attached to the patient will transmit their data simultaneously to the coordinator. In this situation, there is a higher chance of interference due to the communication among the

sensors themselves and between the sensor and the base station. These sensor nodes also suffer from multiple access interference (MAI) due to the poor cross-correlation properties of the spreading sequences used in the network. This MAI depends on the aperiodic correlation properties of the spreading sequences rather than the periodic properties of the sequences [14,15]. Therefore, MAI can be mitigated by having better aperiodic correlation properties in the use of spreading sequences. Hence, polyphase spreading sequences are applied at the physical layer to reduce chip errors. Therefore, the objectives of this paper are as follows:

- To discuss the aperiodic correlation properties for sets of different chip sequences such as binary (PN, Gold, RC7) and polyphase spreading sequences (ZC);
- To find out the relevant chip sequences based on the aperiodic correlation properties;
- To employ the appropriate chip sequences at the physical layer to improve chip errors.

Through MATLAB simulation, it is found that all three binary spreading sequences (PN, Gold, and RC7) degrade the performance of the system, whereas polyphase sequences improve CER significantly in comparison to the binary codes, as described in detail later in this paper.

The rest of the paper is organized as follows: an overview of data packets at the physical layer is provided in Section 2. Section 3 describes the working model of the system. The method of generation and the correlation properties of sequences are also defined in this section. The evaluation of various properties of sequences through exhaustive simulation is presented in Section 4. The comparisons of chip error rate, obtained by using the binary and polyphase sequences at the physical layer, are described in detail. Section 5 summarizes the paper and suggests future work.

## 2. Background

The physical layer of IEEE Std. 802.15.4 incorporates the physical protocol data unit (PPDU) packet structure. All multiple octet fields shall be transmitted or received with the least significant octet first. The PPDU consists of a synchronization header (SHR), physical header (PHR), and physical service data unit (PSDU), as shown in Figure 2. The SHR is used for synchronizing the receiver device onto an incoming bit stream. It consists of two fields, namely the preamble and the start frame delimiter (SFD). The preamble field consists of 4 octets of zeros and is used by the transceiver to synchronize the chip and symbol with an incoming packet from the transmitter. The SFD field indicates the end of the synchronization header and the commencement of the packet data. The length of the SFD field is 1 byte and its value is given in [9,10]. The physical header provides information about frame length, and its size is also 1 byte, of which 7 bits determine the PSDU size and the eighth bit is reserved as zero. PSDU is a variable length payload between 0 and 127 bytes.

| SHR | | PHR | | Physical payload |
|---|---|---|---|---|
| Preamble | SFD | Frame length 7 bits | Reserved 1 bit | PSDU |
| 4 bytes | 1 byte | 1 byte | | 0–127 bytes |

**Figure 2.** PPDU format of physical layer.

The information bits from the PSDU are grouped into groups of 4 bits, known as symbols. Now each symbol is replaced by one of 16 possible chipping sequences with a length of 32 chips each. This way the information bits are mapped into chips and then transmitted after OQPSK modulation. The receiving system compares each received group $R$ of chips to one of 16 possible chipping sequences $S_i$, $(i = 0, \ldots 15)$ used at the

transmitter end by using maximum likelihood (ML) detection. The output of the ML detector is given in Eq. (1) [6].

$$D = \arg\min \{h(R, S_i)\} \tag{1}$$

Here, $h$ is the Hamming distance operator (the number of different locations where the corresponding chips are dissimilar). The lower the value of the Hamming distance operator, the more similar the received group of chips are to the transmitted chip sequences.

## 3. Methodology

In this section, we discuss the main block diagram of the system describing the transmitter with the various blocks, namely the source of information bits, bit to symbol mapper, symbol to chip mapper, modulator, and then receiver section made up of demodulator, chip to symbol mapper, and symbol to bit mapper. We then calculate the chip errors.

### 3.1. Discussion of principal block diagram

At the physical layer, the IEEE 802.15.4 Standard operates in three different frequency bands, including the ISM band (2.45 GHz). There is a single channel (Ch0) operating at a frequency of 868.3 MHz between 868.0 and 868.8 MHz, 10 channels (Ch1–Ch10), operating in the range of 902.0–928.0 MHz, and 16 channels (Ch11–Ch26) between 2400 and 2483.5 MHz. This standard uses the DSSS and offset quadrature phase shift keying (OQPSK) modulation technique to increase the frequency of the signal and reduce the effect of interference from nearby networks operating in the 2.4-GHz band [16,17]. The 2.4-GHz band uses a 250-kbps bit rate and maps each 4 bits of information into symbols, providing a symbol rate of 62.5K symbols per second. Then each symbol is mapped to one of 16 quasiorthogonal PN sequences (standard chip sequences used in [9,10]) for transmission. The PN sequences consist of 32 chips, each making a chip rate of 2 Mcps. The PN sequences for successive data symbols are concatenated and the aggregate chip sequence is then modulated onto the carrier using OQPSK modulation with half-sine pulse-shaping. The half-sine pulse-shaping filter used for each baseband chip is given by Eq. (2).

$$p(t) = \begin{cases} \sin\left(\pi \frac{t}{2T_c}\right) & 0 \le t \le 2T_c \\ 0 & otherwise \end{cases} \tag{2}$$

Here, $T_c$ is the chip duration.

Even-indexed chips are modulated onto the in-phase carrier and odd-indexed chips are modulated onto the quadrature-phase carrier. To form the offset between I-phase and Q-phase chip modulation, Q-phase chips are delayed by $T_c$ with respect to the I-phase chips, where $T_c$ is the inverse of the chip rate. The least significant chip is transmitted first and the most significant chip is transmitted last. The chip sequences are then transmitted through the channel, adding additive white Gaussian noise (AWGN). At the receiver end, the transmitted chips are compared with the received chips by using an ML detector, as given in Eq. (1). The functional block diagram for calculating the chip errors is shown in Figure 3.

### 3.2. Generation of sequences

This paper uses various chip sequences to reduce the chip errors. These chip sequences and their method of generation are provided below.

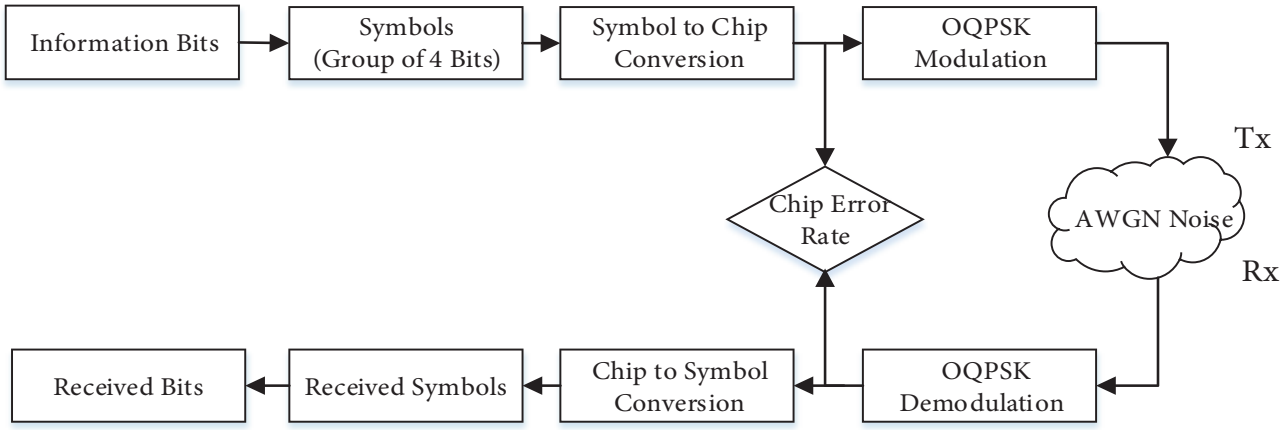


**Figure 3.** Block diagram for calculation of chip error rate.

PN sequences: The standard chip sequences used in [9,10] are pseudonoise (PN) sequences and sequences $S_i$, $(i = 1, \ldots 7)$ generated from $S_0$ by 4 chip circular shifts. $S_i$, $(i = 8, \ldots 15)$ are obtained from the former eight by inversion of odd-indexed chips. The sequences obtained with this method are quasiorthogonal; hence, they do not possess all properties of orthogonal sequences. The PN sequences provide poor synchronization with the receiving packets and cannot withstand real error patterns.

Gold sequences: Gold code sequences are generated by the binary addition (XOR) of two different m-sequences of the same length. The m-sequences are derived by using linear feedback shift registers (LFSR). Only the preferred pair of m-sequences is considered for the generation of Gold codes. From the pair of preferred m-sequences, Gold codes are formed by the modulo 2 sum of one sequence with the shifted versions of the second sequence, or vice versa [11,12].

RC7 sequences: To overcome the shortcomings caused by PN and Gold sequences, RC7 codes were proposed in [6]. In RC7, 8 quadruples are fitted into 32 chips, as shown in Table 1. The last 4 chips in every sequence are made as the inverse of the chip pattern followed in the first 28 chips for RC7 coding. In RC7 codes, the last 4 chips from a 32-chip sequence should act as pattern breakers.

Polyphase sequences: Polyphase sequences are advised here over binary sequences to improve system performance. Polyphase sequences are complex roots of unity, i.e. $b_n = \exp\left(\frac{i2\pi x_n}{q}\right)$, and all members of these sequences have an absolute value of unit magnitude. Various polyphase sequences are available, such as Zadoff Chu (ZC), Oppermann and Vucetic (OV), and analytical bandlimited complex spreading sequences (ABC) [18]. ZC sequences are used in this paper. ZC sequences $\{a_k\}$ of length $N$ can be defined as:

$$a_k = \begin{cases} \exp\left(i\frac{M\pi k^2}{N}\right) & \text{for even } N \\ \exp\left(i\frac{M\pi k(k+1)}{N}\right) & \text{for odd } N \end{cases} \tag{3}$$

where

$$k = 0, \ldots N-1$$

In both cases, $i = \sqrt{-1}$ and $M$ is an integer that is relatively prime to $N$. For length $N = 32$, there are 16 possible ZC sequences that can be generated with this method.

**Table 1.** RC7 chip sequences.

| Symbol | 8 Quadruples | 32-Chip sequence |
|---|---|---|
| 0x0 | 0x0000000F | 0000 0000 0000 0000 0000 0000 0000 1111 |
| 0x1 | 0x1111111E | 0001 0001 0001 0001 0001 0001 0001 1110 |
| 0x2 | 0x2222222D | 0010 0010 0010 0010 0010 0010 0010 1101 |
| 0x3 | 0x3333333C | 0011 0011 0011 0011 0011 0011 0011 1100 |
| 0x4 | 0x4444444B | 0100 0100 0100 0100 0100 0100 0100 1011 |
| 0x5 | 0x5555555A | 0101 0101 0101 0101 0101 0101 0101 1010 |
| 0x6 | 0x66666669 | 0110 0110 0110 0110 0110 0110 0110 1001 |
| 0x7 | 0x77777778 | 0111 0111 0111 0111 0111 0111 0111 1000 |
| 0x8 | 0x88888887 | 1000 1000 1000 1000 1000 1000 1000 0111 |
| 0x9 | 0x99999996 | 1001 1001 1001 1001 1001 1001 1001 0110 |
| 0xA | 0xAAAAAAA5 | 1010 1010 1010 1010 1010 1010 1010 0101 |
| 0xB | 0xBBBBBBB4 | 1011 1011 1011 1011 1011 1011 1011 0100 |
| 0xC | 0xCCCCCCC3 | 1100 1100 1100 1100 1100 1100 1100 0011 |
| 0xD | 0xDDDDDDD2 | 1101 1101 1101 1101 1101 1101 1101 0010 |
| 0xE | 0xEEEEEEE1 | 1110 1110 1110 1110 1110 1110 1110 0001 |
| 0xF | 0xFFFFFFF0 | 1111 1111 1111 1111 1111 1111 1111 0000 |

### 3.3. Properties of sequences

In WSNs, due to multipath propagation delay, the communication among sensor devices and the coordinator is asynchronous in nature. In such systems, MAI also takes place, which degrades the performance of the system. The need for considering the aperiodic correlation properties for an asynchronous DSSS (A-DSSS) is presented in [19–22]. The aperiodic correlation functions of various sequences are described below.

Aperiodic correlation functions: Correlation functions are the key properties used to qualify the spreading sequences. Correlation of sequences is a measurement of the degree of similarity of one sequence to the shifted versions of itself or to other sequences. The aperiodic cross-correlation functions (ACCF) of a pair of polyphase sequences $u_X$ and $u_Y$ are expressed in Eq. (4) [23]:

$$C_{XY}(l) = \begin{cases} \sum_{k=0}^{N-1-l} u_X(k)\, u_Y^*(k+l) & 0 \le l \le N-1 \\ \sum_{k=0}^{N-1+l} u_X(k-l)\, u_Y^*(k) & 1-N \le l < 0 \\ 0 & elsewhere \end{cases} \tag{4}$$

where $*\}$ represents the complex conjugate and $N$ is the sequence length. If $u_X$ and $u_Y$ are same sequences, then $C_{XX}(l)$ will be an aperiodic autocorrelation function. Ideally, the value of aperiodic cross-correlation must be zero for the nonzero time shifts to combat the effects of MAI; however, this is not possible. Therefore, we have to choose that set of sequences for which the value of ACCF is minimum. The ACCF between a pair of binary sequences $b_n$ and $c_n$ is given by Eq. (5) [24].

$$C_{k,j}(\tau) = \begin{cases} \sum_{n=0}^{N-1-\tau} b_n c_{n+\tau} & 0 \le \tau \le N-1 \\ \sum_{n=0}^{N-1+\tau} b_{n-\tau} c_n & 1-N \le \tau < 0 \\ 0 & \tau > N \end{cases} \tag{5}$$

Here, N is the length of the sequence. Since PN, Gold, and RC7 are all binary sequences, Eq. (5) is equally applicable to these sequences.

Merit factor: The merit factor $F$ of a sequence is defined as the ratio of energy in the main lobe to the energy in the side lobes of the aperiodic autocorrelation function (AACF) [24,25].

$$F = \frac{|C_k(0)|^2}{2\sum_{\tau=1}^{N-1}|C_k(\tau)|^2} \tag{6}$$

Here, $c_k$ is the AACF of a binary or polyphase sequence. In this equation, $F$ is inversely proportional to the energy in the side lobes. Therefore, to achieve a high value of merit factor, the value of the AACF must be zero for the out-of-phase time shifts. In addition, the side lobes of the AACF indicate energy inefficiency, so their values must be minimum.

Energy efficiency: This property is of main concern for WSNs, because these networks require high energy efficiency for their long-term operation. Several energy conservation schemes were discussed in [26]. The energy efficiency $(\eta)$ of the sequences is described by Eq. (7), given below [24]:

$$\eta = \frac{\sum_{k=0}^{N-1}|a_k|^2}{N\,max\left(|a_k|^2\right)} \tag{7}$$

where $a_k$ may be a binary or polyphase sequence. Using such sequences, which are energy-efficient in themselves, can make the system more energy-efficient.

## 4. Results and discussion

### 4.1. Simulation parameters

The various parameters considered for evaluating the system performance in MATLAB are provided in Table 2.

**Table 2.** System parameters.

| Parameters | Values |
|---|---|
| No. of octets from PSDU | 127 |
| No. of octets from header | 6 |
| Total no. of bits | 1064 |
| Symbols | 266 |
| No. of samples/bit | 10 |
| Carrier frequency | 2.45 GHz |
| Modulation | OQPSK |

### 4.2. Evaluation of correlation properties of different sequences

As mentioned in Section 3.3, aperiodic correlation properties play an important role in determining the performance of A-DSSS systems. The aperiodic correlation properties of different sequences are evaluated by MATLAB simulation.

Aperiodic cross-correlation function: The normalized aperiodic cross-correlations of PN, Gold, RC7, and ZC sequences are shown in Figure 4. Three random pairs of sequences are considered for the simulation.

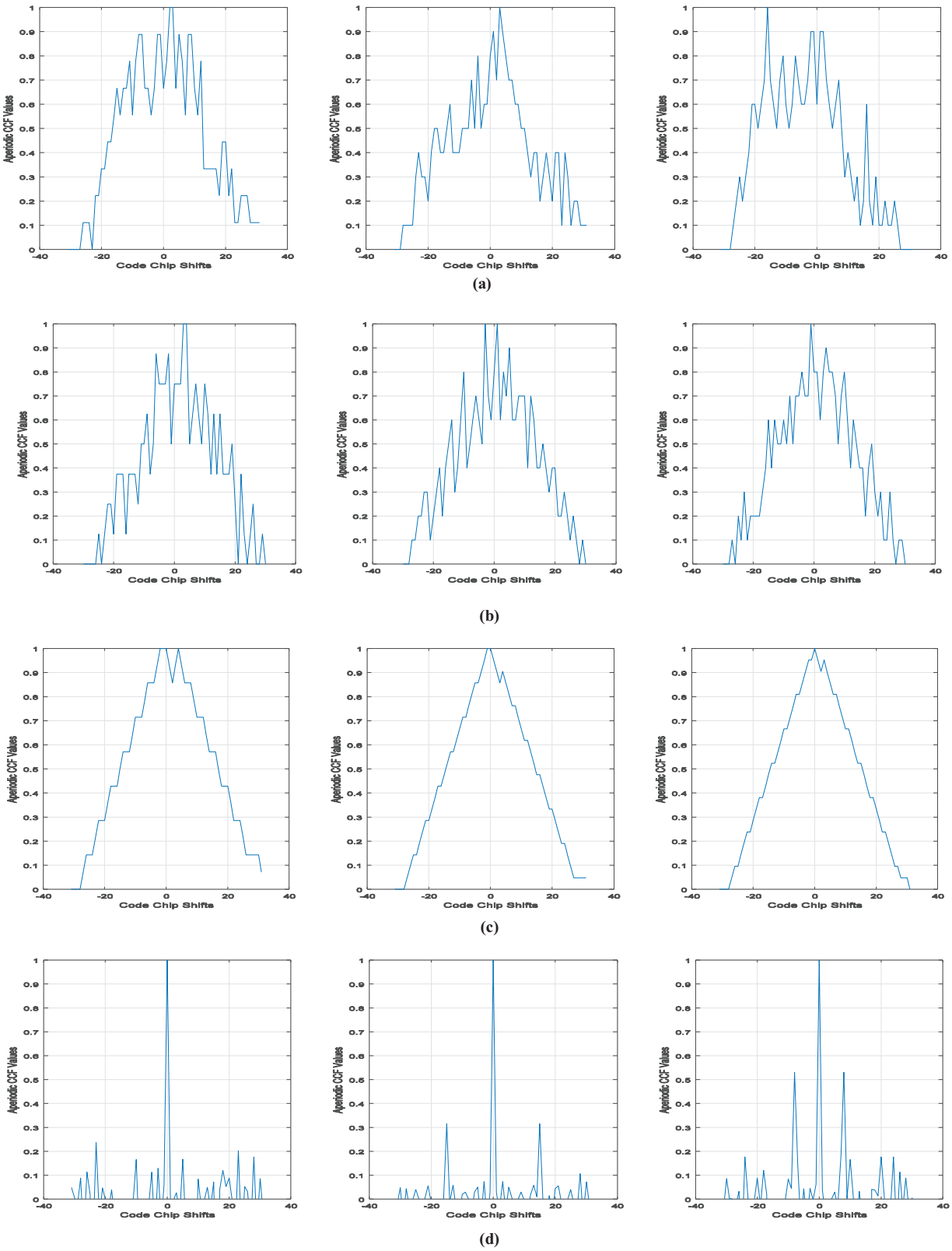


**Figure 4.** Aperiodic cross-correlation function of (a) PN sequences, (b) Gold sequences, (c) RC7 sequences, (d) ZC sequences.

From Figure 4, it is clear that the side lobe peaks of the ACCF are very small for ZC sequences in comparison to PN, Gold, and RC7 sequences. The value of side lobe peaks of the ACCF varies between 0 and 0.52 (highest) in the case of ZC sequences, whereas it ranges from 0 to 0.9 in the case of PN and RC7 sequences and rises to 1 for Gold sequences. In order to compare the binary and polyphase sequences, the mean of their ACCF is calculated in Figure 4 and is shown in Table 3. Higher values of mean aperiodic cross-correlation imply that binary sequences are highly correlated with each other and hence degrade the performance of the system.

**Table 3.** Mean value of aperiodic cross-correlation of sequences.

| PN | Gold | RC7 | ZC |
|---|---|---|---|
| 0.4515 | 0.3934 | 0.5079 | 0.0317 |
| 0.4063 | 0.4197 | 0.4656 | 0.0224 |
| 0.4063 | 0.4197 | 0.4656 | 0.0317 |

In Table 3, it is shown that ACCF values of ZC sequences are approximately 93% lower than those of binary sequences. This means that the ZC sequences improve system performance to a greater extent than binary sequences.

Aperiodic autocorrelation function: The normalized aperiodic autocorrelations of PN, Gold, RC7, and ZC sequences are shown in Figure 5. ZC sequences have lower side lobe peaks of AACF in comparison to binary sequences, which make them highly energy-efficient and also allow them to have high values of merit factor. The value of the merit factor for ZC sequences is computed as 3.7529, whereas for PN, Gold, and RC7 sequences it is 0.2008, 0.2131, and 0.2301, respectively. ZC sequences have a 94% higher merit factor than binary sequences. According to Eq. (7), it has been observed that ZC sequences are 100% energy-efficient (because of their constant magnitude), whereas other sequences only have 50% energy efficiency.

For A-DSSS systems, it is desirable to have minimum values of ACCF, out-of-phase peaks of AACF, and maximum value of merit factor. These criteria are fulfilled by ZC sequences; therefore, ZC sequences are highlighted here for safety- and mission-critical applications of WSNs to increase communication reliability.

### 4.3. Performance evaluation

Bit error rate (BER) and packet reception rate (PRR) have been studied by various researchers in [27–30] employing only standard PN sequences. Several research articles highlighted chip and symbol errors and their causes in different environments, such as interference from networks operating in the same 2.4-GHz band, multipath fading, and attenuation [31,32]. The comparison of chip error rate (CER), obtained by employing PN, Gold, RC7, and ZC sequences at the physical layer of IEEE Std. 802.15.4, is given in Figure 6. The values of CER for different sequences at an SNR of 1.85 dB is shown in Table 4, where it is proven that ZC sequences have lower CER in comparison to other sequences. In the case of ZC sequences, CER is reduced to zero at an SNR of 1.85 dB, whereas for binary sequences, it becomes zero at an SNR of 2.35 dB, which shows the superiority of ZC sequences over other sequences. In such applications of WSNs, where data reliability and energy efficiency have the highest degree of importance, polyphase sequences must be used.

## 5. Conclusion and future work

To fulfill the requirements of communication reliability and energy efficiency for safety/mission-critical WSNs, polyphase-spreading sequences are used in this paper. They are also compared with formal binary sequences (PN, Gold, and RC7). ZC sequences provide 75% less chip error than binary sequences. In addition, ZC

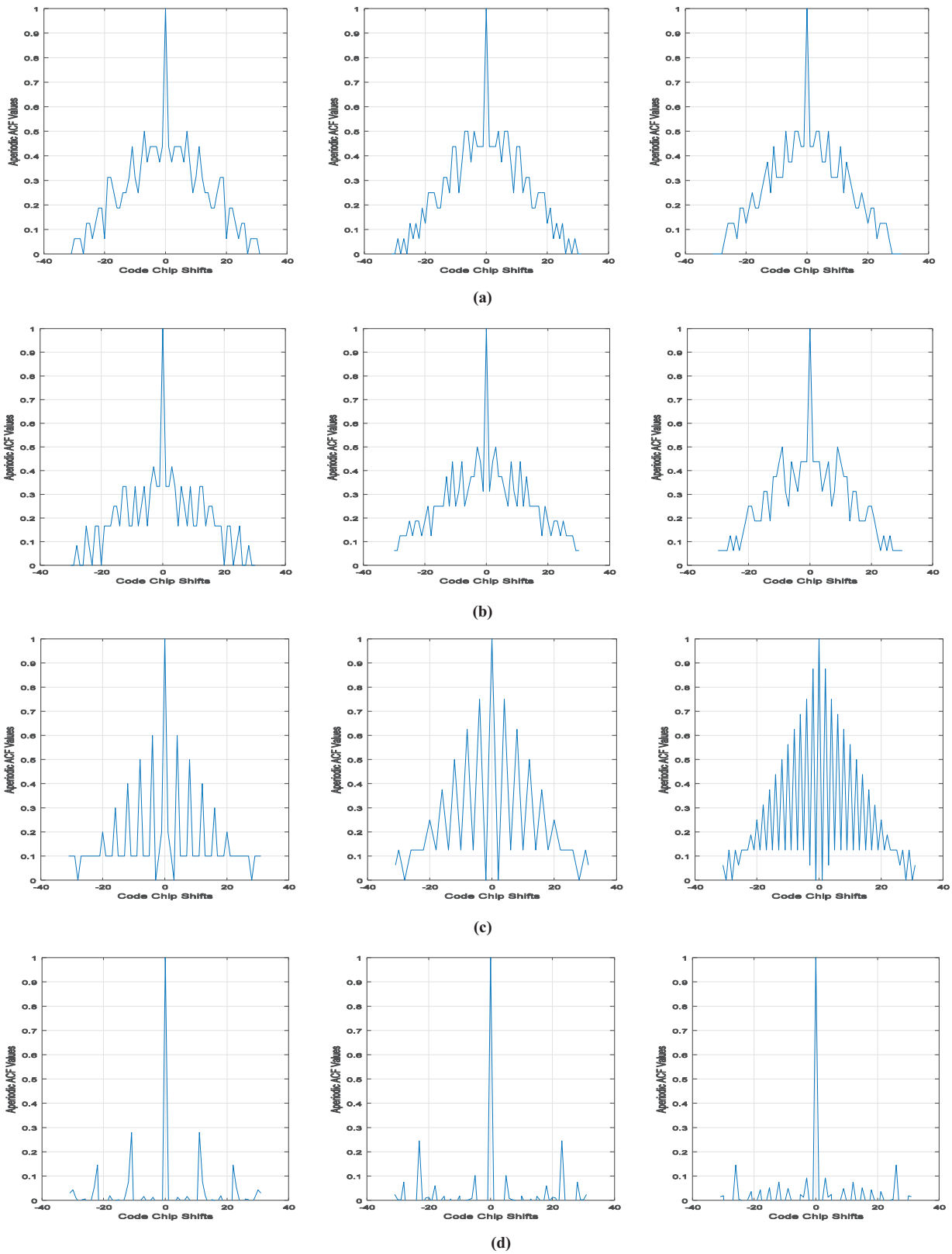


**Figure 5.** Aperiodic autocorrelation function of (a) PN sequences, (b) Gold sequences, (c) RC7 sequences, (d) ZC sequences.

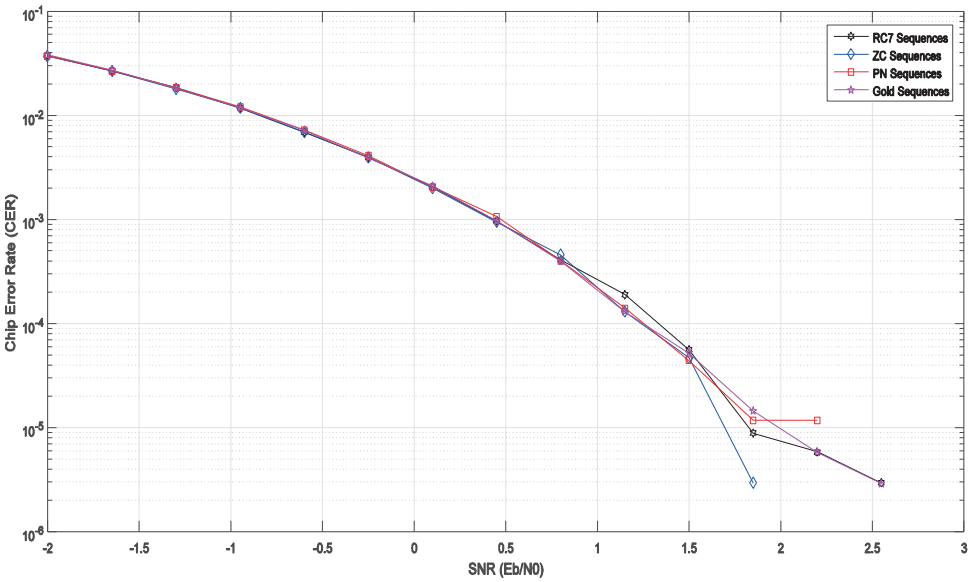


**Figure 6.** Chip error rate evaluation for various sequences.

**Table 4.** CER for sequences at SNR of 1.85 dB.t

| Chip sequences | CER |
|---|---|
| PN | $1.18 \times 10^{-5}$ |
| Gold | $1.45 \times 10^{-5}$ |
| RC7 | $0.91 \times 10^{-5}$ |
| ZC | $2.94 \times 10^{-6}$ |

sequences were found to be 100% energy-efficient; other sequences have only 50% energy efficiency. Besides these advantages, ZC sequences possess the limitation of complexity, as they make the system a little more complex in nature. This is the only limitation of ZC sequences, which will be overcome in the near future.

## References

[1] Dargie WW, Poellabauer C. Fundamentals of Wireless Sensor Networks: Theory and Practice. Hoboken, NJ, USA: Wiley, 2010.

[2] Zheng J, Jamalipour A. Wireless Sensor Networks: A Networking Perspective. Hoboken, NJ, USA: Wiley, 2009.

[3] Akyildiz IF, Su W, Sankarasubramaniam Y, Cayirci E. Wireless sensor networks: a survey. Comput Netw 2002; 38: 393-422.

[4] Chong CY, Kumar SP. Sensor networks: evolution, opportunities, and challenges. Proc IEEE 2003; 918: 1247-1256.

[5] Gaddam A, Mukhopadhyay SC, Sen Gupta G, Guesgen H. Wireless sensors networks based monitoring: review, challenges and implementation issues. In: IEEE 2008 International Conference on Sensing Technology; 30 November–3 December 2008; Tainan, Taiwan. New York, NY, USA: IEEE. pp. 533-538.

[6] Barac F, Gidlund M, Zhang T. CLAP: Chip-level augmentation of IEEE 802.15.4 PHY for error-intolerant WSN communication. In: IEEE 2015 Vehicular Technology Conference; 11–14 May 2015; Glasgow, UK. New York, NY, USA: IEEE. pp. 1-7.

[7] Wu K, Tan H, Ngan HL, Liu Y, Ni LM. Chip error pattern analysis in IEEE 802.15.4. IEEE T Mobile Comput 2012; 11: 543-552.

[8] Fang S, Berber S, Swain A, Rehman SU. A study on DSSS transceivers using OQPSK modulation by IEEE 802.15.4 in AWGN and flat Rayleigh fading channels. In: IEEE 2010 TENCON Conference; 21–24 November 2010; Fukuoka, Japan. New York, NY, USA: IEEE. pp. 1347-1351.

[9] IEEE. IEEE Standard (802.15.4-2006) for Information Technology-Telecommunication and Information Exchange Between Systems—Local and Metropolitan Area Networks—Specific Requirements, Part 15.4: Wireless Medium Access Control (MAC) and Physical Layer (PHY) Specifications for Low-Rate Wireless Personal Area Networks (WPANs). New York, NY, USA: IEEE, 2006.

[10] IEEE. IEEE Standard (802.15.4-2003) for Information Technology-Telecommunications and Information Exchange Between Systems—Local and Metropolitan Area Networks—Specific Requirements, Part 15.4: Wireless Medium Access Control (MAC) and Physical Layer (PHY) Specifications for Low-Rate Wireless Personal Area Networks (WPANs). New York, NY, USA: IEEE, 2003.

[11] IEEE. 802.15.4k - IEEE Standard for Local and Metropolitan Area Networks— Part 15.4: Low Rate Wireless Personal Area Networks (LR-WPANs). Amendment 5: Physical Layer Specifications for Low Energy, Critical Infrastructure Monitoring Networks. New York, NY, USA: IEEE, 2013.

[12] Xiong X, Wu T, Long H, Zheng K. Implementation and performance evaluation of LECIM for 5G M2M applications with SDR. In: IEEE 2014 Globecom Workshop; 8–12 December 2004; Austin, TX, USA. New York, NY, USA: IEEE. pp. 612-617.

[13] Tang X, Xu R. Code and carrier synchronization for IEEE 802.15.4K DSSS PHY. In: Park JH, Stojmenovic I, Jeong HY, Yi G, editors. Computer Science and Its Applications. London, UK: Taylor and Francis, 2015. pp. 149-154.

[14] Wysocki BJ, Wysocki TA. On a method to improve correlation properties of orthogonal polyphase spreading sequences. J Telecommun Inf Technol 2003; 2: 99-105.

[15] Chan CK, Lam WH. A simplified aperiodic cross-correlation model for direct-sequence spread-spectrum multiple-access communication systems. In: IEEE 1994 International Conference on Communications; 1–5 May 1994; Lannion, France. New York, NY, USA: IEEE. pp. 1516-1520.

[16] Jin Y, Al Ameen M, Liu H, Kwak KS. Interference mitigation study for low energy critical infrastructure monitoring applications. In: IEEE 2012 International Symposium on Communications and Information Technologies; 2–5 October 2012; Gold Coast, Australia. New York, NY, USA: IEEE. pp. 962-966.

[17] Çöplü T, Oktuğ SF. PRESCIENT: A predictive channel access scheme for IEEE 802.15.4-compliant devices considering IEEE 802.11 coexistence. Turk J Elec Eng & Comp Sci 2015; 23: 1465-1478.

[18] Jamil M, Linde LP. A comparison of unfiltered and filtered complex spreading sequences based on aperiodic correlation properties. In: IEEE 1998 International Symposium on Spread Spectrum Techniques and Applications; 4 September 1998; Sun City, South Africa. New York, NY, USA: IEEE. pp. 686-691.

[19] Anderson D, Wintz PA. Analysis of a spread-spectrum multiple-access system with a hard limiter. IEEE T Commun Techn 1969; 17: 285-290.

[20] Pursley MB. Performance evaluation for phase-coded spread-spectrum multiple-access communication. Part I: System analysis. IEEE T Commun 1977; 25: 795-799.

[21] Karkkainen KH, Leppanen PA. Comparison of the performance of some linear spreading code families for asynchronous DS/SSMA systems. In: IEEE 1991 Military Communications Conference; 4–7 November 1991; Maclean, VA, USA. New York, NY, USA: IEEE. pp. 784-790.

[22] Chen XH, Lang T, Oksman J. Multiple chip-rate DS/CDMA system and its spreading code dependent performance analysis. IEE P-Commun 1998; 145: 371-377.

[23] Oppermann I, Vucetic BS. Complex spreading sequences with a wide range of correlation properties. IEEE T Commun 1997; 45: 365-375.

[24] Khan Z. Performance analysis of spreading sequences in radio channels. PhD, Blekinge Institute of Technology, Karlskrona, Sweden.

[25] Borwein PE, Ferguson R, Knauer J. The merit factor problem. Lond Math S 2000; 52-70.

[26] Solaiman B F, Sheta A. Energy optimization in wireless sensor networks using a hybrid K-means PSO clustering algorithm. Turk J Elec Eng & Comp Sci 2016; 24: 2679-2695.

[27] Shuaib K, Alnuaimi M, Boulmalf M, Jawhar I, Sallabi F, Lakas A. Performance evaluation of IEEE 802.15.4: experimental and simulation results. J Commun 2007; 2: 29-37.

[28] Xia J, Chen L, Li Y, Zhou Y. System modeling and analysis of the IEEE 802.15. 4 physical layer design. In: IEEE 2011 International Conference on ASIC; 25–28 October 2011; Xiamen, China. New York, NY, USA: IEEE. pp. 228-231.

[29] Anwar AK, Lavagno L. Simulink modeling of the 802.15.4 physical layer for model-based design of wireless sensor networks. In: IEEE 2009 International Conference on Sensor Technologies and Applications; 18–23 June 2009; Athens, Greece. New York, NY, USA: IEEE. pp. 38-42.

[30] Velagapudi P, Eravatri BC, Mantri MB, Mani VV. Performance analysis of various IEEE 802.15.4 PHYs under Rayleigh fading channel. In: IEEE 2013 International Conference on Advanced Computing and Communication Systems; 19–21 December 2013; Sri Eshwar, India. New York, NY, USA: IEEE. pp. 1-5.

[31] Barac F, Gidlund M, Zhang T. Scrutinizing bit- and symbol-errors of IEEE 802.15.4 communication in industrial environments. IEEE T Instrum Meas 2014; 63: 1783-1794.

[32] Planin P, Pesovic U, Gleich D. Chip error probability of IEEE 802.15.4 wireless transmission. In: IEEE 2014 International Electrotechnical and Computer Science Conference; 22–24 September 2014; Potroroz, Slovenia. New York, NY, USA: IEEE. pp. 65-68.